

# New sarcosine-metal halide complexes related to the ferroelectric TSCC

Rebecca Clulow and Philip Lightfoot\*

School of Chemistry and EaStChem, University of St Andrews, St Andrews, Fife, KY16 9ST, UK

\*E-mail: pl@st-andrews.ac.uk

## Abstract

There are relatively few sarcosine metal halide complexes. Of these, *tris* sarcosine calcium chloride (TSCC)  $((C_3NO_2H_7)_3CaCl_2)$  stands out as an unusual example of a molecular ferroelectric. Here we report the syntheses of eight new related sarcosine-metal halide complexes by slow evaporation. The newly reported materials can be categorised into four different structure types, *viz.* 3:1 complexes such as  $(C_3NO_2H_7)_3CaBr_2$ , hydrated 3:1 complexes such as  $(C_3NO_2H_7)_3MnI_2 \cdot 2H_2O$ , hydrated 2:1 complexes such as  $(C_3NO_2H_7)_2MgCl_2 \cdot 2H_2O$ , and a 4:1 complex  $(C_3NO_2H_7)_4CaI_2 \cdot 2H_2O$ . The crystal structures of all examples have been determined at multiple temperatures but no evidence is found for any structural transitions to polar phases, either by single crystal X-ray diffraction or by differential scanning calorimetry. The specific compositional reasons behind the apparently unique ferroelectric behaviour of TSCC therefore remain to be ascertained.

## Introduction

Ferroelectrics have a wide range of technological applications including in thermal detectors, capacitors and memory devices.<sup>1,2</sup> However, the inclusion of heavy metals poses several problems surrounding their toxicity, sustainability and cost. Organic or metal-organic ferroelectrics may offer a more benign and cheaper alternative, in addition to offering other attractive properties such as lightness, flexibility and tunability.<sup>3</sup> The first example of a ferroelectric crystal was Rochelle salt  $(KNaC_4H_4O_6 \cdot 4H_2O)$  which was discovered in 1921.<sup>4</sup> Despite its discovery nearly a century ago, there were relatively few early examples of metal-organic ferroelectrics and these were soon superseded by purely inorganic oxides.

More recently, interest in molecular-based ferroelectrics has enjoyed a resurgence<sup>1,3,5</sup>. Amino acids are one of the prevalent families of prospective metal-organic ferroelectrics, since they are benign, water soluble and display large structural diversity<sup>6</sup>. The sarcosine molecule can exist in the zwitterionic form, the protonated, cation form or deprotonated, anionic form. The most well-known example is *tris*-sarcosine calcium chloride (TSCC), which is known to have ferroelectric properties below  $T_c \sim 130$  K<sup>7</sup>. At  $T_c$  TSCC undergoes a second order displacive phase transition from the centrosymmetric  $Pnma$ <sup>8</sup> to the polar  $Pn2_1a$  space group.<sup>9</sup> The unit cell metrics of both phases are approximately  $a \sim 9.2$ ,  $b \sim 17.5$ ,  $c \sim 10.3$  Å. The crystal structure consists of distorted  $CaO_6$  octahedra which are linked by (O,O') sarcosine bridging ligands to form infinite chains along the  $a$  axis. These chains are interconnected by N-H...Cl hydrogen bonds to form the three dimensional pseudo-hexagonal structure (Figure 1).

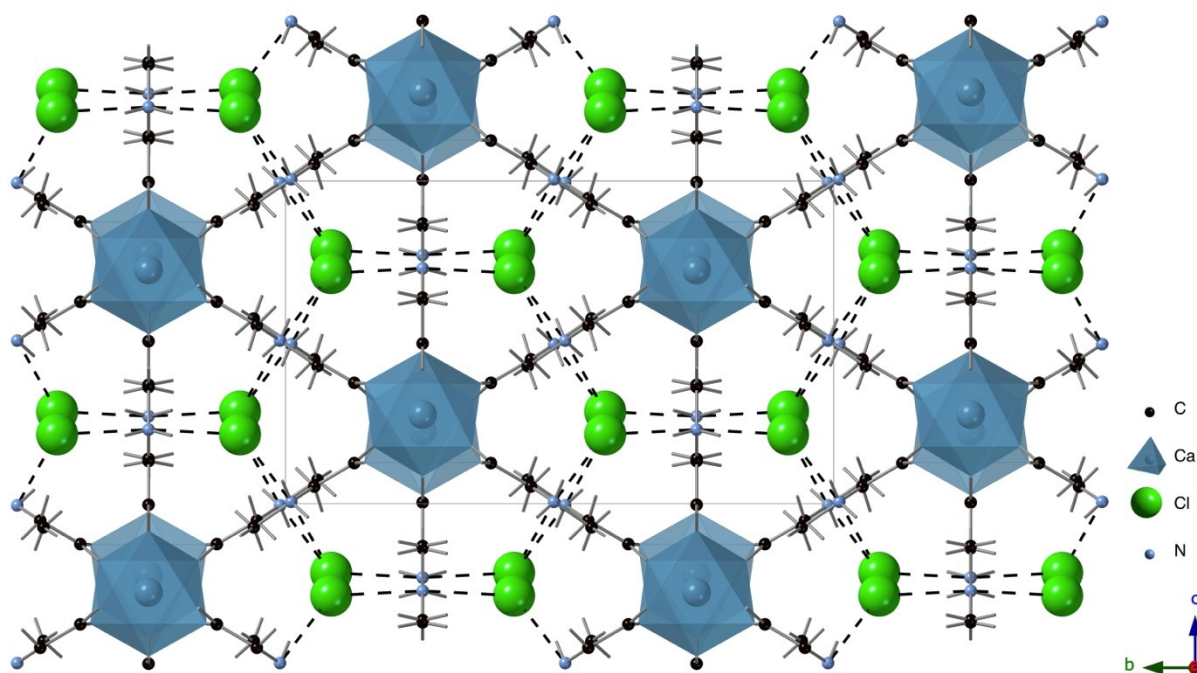


**Figure 1** Structure of TSCC ( $(\text{C}_3\text{NO}_2\text{H}_7)_3\text{CaCl}_2$ ) viewed along the  $a$  axis

TSCC is already one of the most extensively studied amino acid-based ferroelectrics, but much of the research has concerned the physical characterisation of the ferroelectric phase transition itself<sup>10,11</sup>. We have recently carried out a detailed crystallographic study of this phase transition<sup>12</sup>, which shows some unique features; TSCC is best described as a ferrielectric. It is clearly of interest to study derivatives and close analogues of TSCC, in order to further probe the nature of this unusual ferroelectric behaviour and also the potential for realising genuinely useful physical properties in these systems. So far, these developments have largely been restricted to doping of bromide or iodide into TSCC. The substitution of chloride by bromide or iodide is known to suppress the transition temperature to 0 K at 24 %<sup>13</sup> and 72 %<sup>14</sup> doping, respectively. Whilst the effect of halogen substitution has been previously investigated, there has been little research regarding the role of the metal cation. So far, TSCC is the only sarcosine-containing compound in which ferroelectric properties have been demonstrated. Here we report the syntheses and crystal structures of several new TSCC derivatives. Our strategy has been to carry out a more exploratory synthetic survey of sarcosine:MX<sub>2</sub> compositions, where M is a group II cation and X = Cl, Br, I, at a variety of sarcosine:salt ratios.

## Experimental Section

The compounds were synthesised from an aqueous solution by slow evaporation at room temperature using commercially available reagents of at least 98% purity. Sarcosine and the appropriate metal halides were dissolved in stoichiometric quantities in distilled water and after approximately six days, high quality crystals were formed. The resulting crystals were filtered and dried overnight at 50 °C before analysis by X-ray diffraction and differential scanning calorimetry (DSC). Powder X-ray diffraction data were collected on a PANalytical EMPYREAN diffractometer using Cu  $K\alpha_1$  ( $\lambda = 1.5406$  Å) radiation to confirm the purity of each sample. A NETZSCH DSC 204 instrument was used to collect DSC data between 293 K and 103 K at a ramp rate of 5 K/min. TGA data were collected on a STA-780



	2.361(7)	2.564(4)	2.570(5)	2.203(4)	2.094(5)	2.338(5)	2.075(3)	2.323(5)	2.333(5)
	2.379(5)	2.579(4)	2.587(5)	2.209(5)	2.094(5)	2.380(8)	2.105(4)	2.394(5)	2.393(5)
	2.379(5)	2.745(4)	2.656(5)	2.209(5)	2.110(7)	2.380(8)	2.105(4)	2.394(5)	2.393(5)
		2.782(4)	2.937(6)						
N-H-X	3.287(3)	3.174(5)	3.296(5)	3.515(4)	3.318(5)	3.499(6)	3.130(4)	3.558(7)	
	3.321(6)	3.229(5)	3.357(6)	3.565(6)	3.437(7)	3.481(6)	3.098(5)	3.621(7)	
	3.336(7)	3.189(5)	3.305(6)	3.709(5)	3.487(7)			3.604(8)	
		3.245(5)	3.386(6)					3.514(8)	
		3.232(5)	3.327(6)						
		3.259(5)	3.329(6)						
BVS	2.25	2.05	2.05	2.04	2.11	2.13	2.09	2.23	2.18

### 1. Anhydrous 3:1 compositions

Three of the newly synthesised derivatives belong to this first group of structures, which maintain the stoichiometry of the parent compound TSCC. Amongst these, *tris*-sarcosine calcium bromide, TSCB ( $(C_3NO_2H_7)_3CaBr_2$ ) is isostructural to TSCC. Whilst the dielectric properties of TSCB have been previously investigated,<sup>14,15</sup> its crystal structure has never been reported. The compound crystallises in the orthorhombic space group *Pnma*. The crystal structure consists of slightly distorted  $CaO_6$  octahedra with each  $Ca^{2+}$  coordinated to six different sarcosine molecules (Figure 2). The Ca-O bond angles vary between 2.288(5) Å and 2.379(5) Å which is shorter than expected for  $Ca^{2+}$  in six fold coordination, as suggested by the relatively high resultant bond valence sum for Ca. The structure contains two inequivalent sarcosine sites, the first lies on the mirror plane perpendicular to the *b* axis and the second sits on a general position. Each of the  $CaO_6$  octahedra are connected to the next *via* three sarcosine molecules, which act as bridging ligands to form infinite chains along the *a* axis (Figure 2). The resulting *a* axis channels are occupied by the bromide ions and the octahedral chains are interconnected by weak N-H---Br hydrogen bonding. The bromide ions each form three hydrogen bonds to different sarcosine molecules. The introduction of bromine does not cause any significant changes to the crystal structure at 173 K. Despite the similarities between the structures of TSCB and TSCC, there was no evidence of a phase transition to the polar *Pn2<sub>1</sub>a* space group in differential scanning calorimetry (DSC) data down to 90 K.

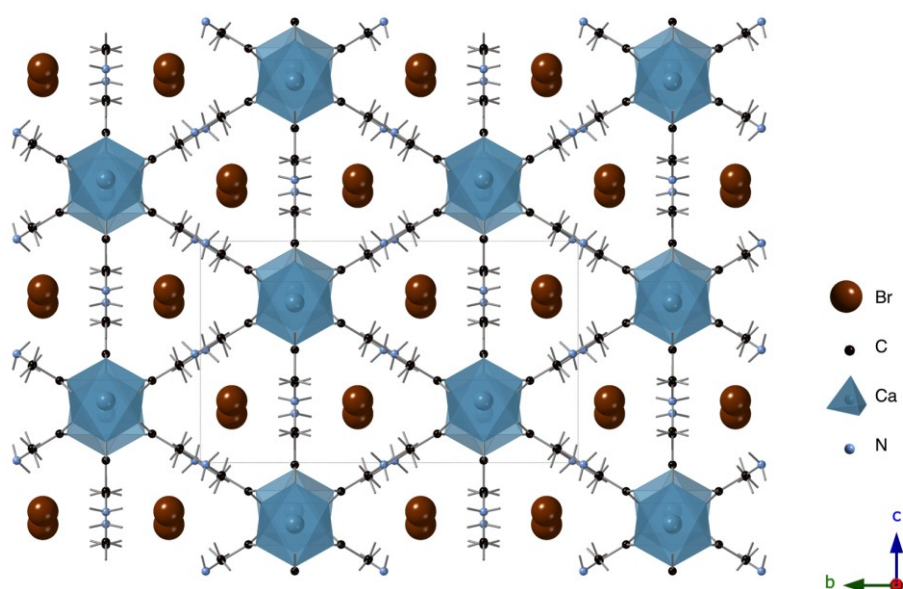


**Figure 2** Structure of TSCB ( $(C_3NO_2H_7)_3CaBr_2$ ) viewed along the *a* axis

Two further derivatives with the same 3:1 stoichiometry, TSSC ( $(C_3NO_2H_7)_3SrCl_2$ ) and TSSB ( $(C_3NO_2H_7)_3SrBr_2$ ), were also synthesised. Whilst the pseudo-hexagonal symmetry and overall

topology of the structures seen in TSCC and TSCB has been maintained, there are significant changes in connectivity and crystal-packing due to the substitution of  $\text{Ca}^{2+}$  with the larger  $\text{Sr}^{2+}$ . These differences are caused by an increase in the coordination number of the metal centre from six to seven, with Sr-O bond distances ranging from 2.433(4) Å to 2.937(6) Å. Each of the  $\text{SrO}_7$  polyhedra shares one oxygen atom with its neighbouring metal centre; as a result, the polyhedra exhibit corner sharing (see Figure 10 for a comparative summary of all the chain architectures).

The structure of TSSC has many similarities to that of TSCC (Figure 3). However, the connectivity of the polyhedra has been altered slightly by the incorporation of the larger  $\text{Sr}^{2+}$  cations, and the resultant crystal symmetry has been lowered from orthorhombic to monoclinic, space group  $P2_1/a$ . Nevertheless, the polyhedra remain connected by the carboxylic acid groups of the sarcosine molecules to form infinite chains along one axis and the overall unit cell metrics remain comparable. Additionally, the hydrogen bonding network has not been disrupted and the polyhedral chains remain interconnected by N-H...Cl bonds. In contrast with the structure of TSCC, the asymmetric unit incorporates three inequivalent sarcosine molecules, on general positions (i.e. each with a multiplicity of four). A similar crystal structure has been reported for the analogue  $(\text{C}_3\text{NO}_2\text{H}_7)_3\text{BaBr}_2$  previously; that structure adopts a similar symmetry and unit cell parameters ( $P2_1/c$ ,  $a = 18.345(4)$  Å,  $b = 10.668(2)$  Å,  $c = 8.9212(18)$  Å,  $\beta = 91.86(3)^\circ$ ) but the inclusion of an even larger cation,  $\text{Ba}^{2+}$ , results in nine-fold coordination around the metal centre.

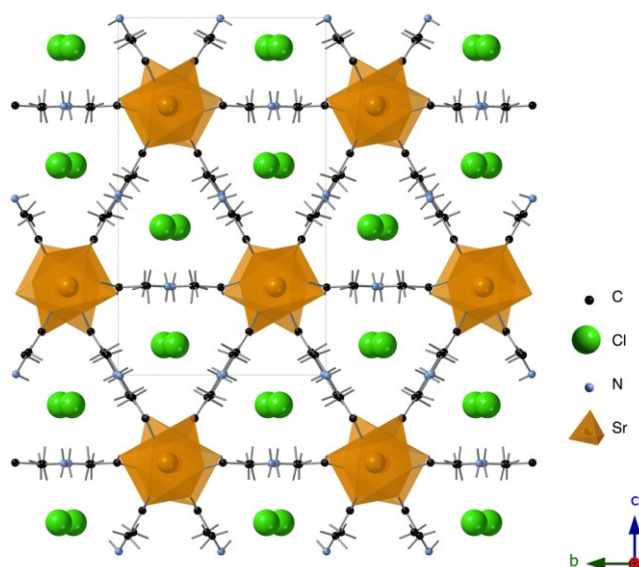


**Figure 3** Structure of TSSC  $((\text{C}_3\text{NO}_2\text{H}_7)_3\text{SrCl}_2)$  viewed along the  $a$  axis

The brominated version, TSSB, was also synthesised. Interestingly, despite the similarities to the previously synthesised derivatives, there is a key change in the crystal packing and resultant unit cell parameters and space group, with one unit cell axis effectively doubled relative to that of TSCC (Table 1). In TSSB the space group is also modified to  $Pcab$ . As observed in TSSC, there are three inequivalent sarcosine molecules, in this case each with a multiplicity of eight. The  $\text{Sr}^{2+}$  cation is coordinated to seven oxygens, one of which is shared with the adjacent  $\text{SrO}_7$  polyhedra. The remaining six oxygens act as bridging ligands to the neighbouring polyhedra resulting in an infinite chain structure along the  $a$  axis (Figure 4). The unit cell doubling is the result of differing orientations of the  $\text{SrO}_7$  polyhedra (Figure 5); when viewed along the  $b$  axis, each of the polyhedral chains are tilted in a different direction. One of the seven Sr-O bonds is significantly longer than the others, 2.937(6) Å compared with  $\sim 2.5$  Å, and is involved in the corner sharing between adjacent polyhedra. Weak N-H...Br hydrogen bonding is again present.

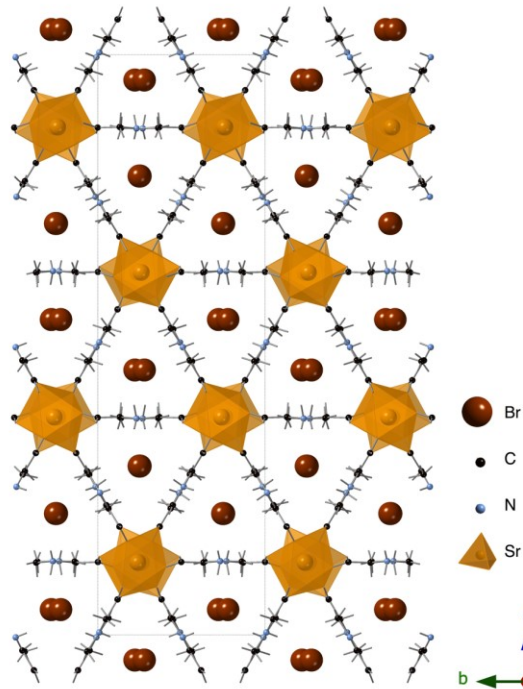


**Figure 4** Structure of TSSB  $((\text{C}_3\text{NO}_2\text{H}_7)_3\text{SrBr}_2)$  viewed along the  $a$  axis

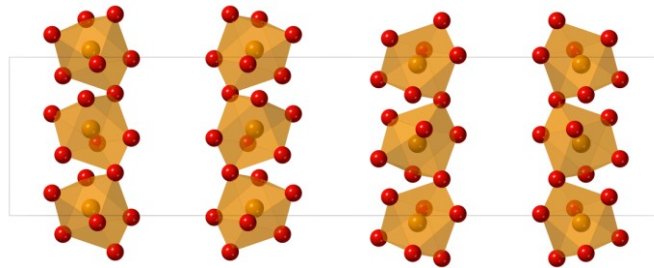


**Figure 5** TSSB: corner-linked  $\text{SrO}_7$  polyhedra form chains along the  $a$  axis

Solid solutions of TSCC-TSSC and TSCB-TSSB were also synthesised using the same method and the incorporation of strontium was confirmed by single crystal X-ray diffraction data. The structures of both 50% strontium-containing compositions (*viz.*  $(\text{C}_3\text{NO}_2\text{H}_7)_3\text{Ca}_{0.5}\text{Sr}_{0.5}\text{Cl}_2$  and  $(\text{C}_3\text{NO}_2\text{H}_7)_3\text{Ca}_{0.5}\text{Sr}_{0.5}\text{Br}_2$ ) derived from single crystal were very similar to the pure calcium-containing derivatives. In both cases, only minor changes are observed in the unit cell parameters with elongation along the  $b$  and  $c$  axes and a slight contraction along the  $a$  axis. The Ca/Sr-O bond lengths increase from an average of 2.335 Å in the pure calcium derivatives to an average of 2.389 Å in the 50% Sr-containing derivatives. The occupancies of the metal sites for both compositions were refined to 56.6(6) % Ca for  $(\text{C}_3\text{NO}_2\text{H}_7)_3\text{Ca}_{0.5}\text{Sr}_{0.5}\text{Cl}_2$  and 60.5(6) % Ca for  $(\text{C}_3\text{NO}_2\text{H}_7)_3\text{Ca}_{0.5}\text{Sr}_{0.5}\text{Br}_2$ . Interestingly, DSC data suggest that the incorporation of low concentrations of strontium in the TSCC structure does not suppress the ferroelectric transition temperature  $T_C$  towards zero, as previously observed for bromide and iodide doping<sup>14,13</sup>. In this case  $T_C$  remains  $\sim 130$  K at low concentrations of strontium, but above 30% strontium the phase transition is no longer observable in DSC data (Figure 6).

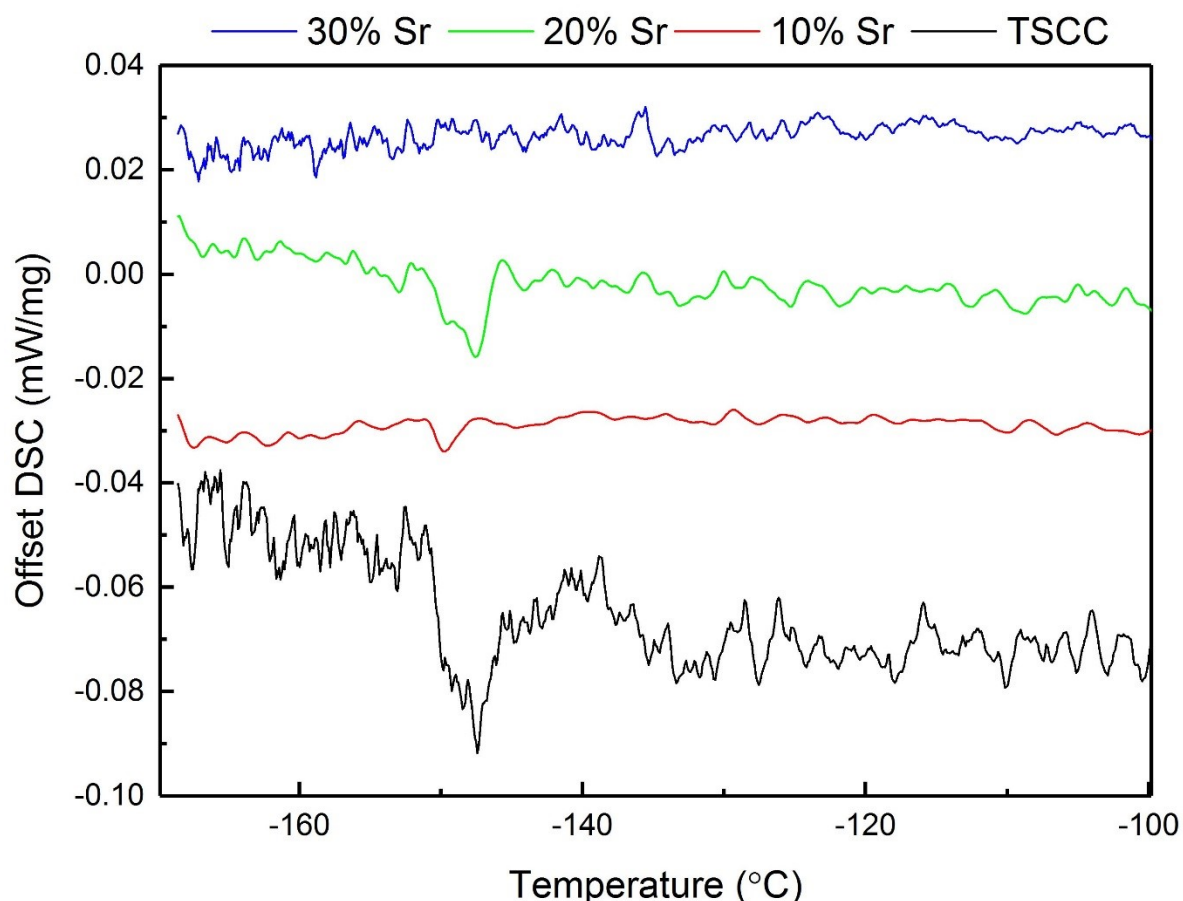


**Figure 6** DSC data for TSCC ( $(C_3NO_2H_7)_3CaCl_2$ ) and strontium doped TSCC

## 2. Hydrated 3:1 compositions

Similar reactions aimed at preparing analogues of TSCC using smaller divalent cations,  $Mn^{2+}$  and  $Mg^{2+}$ , resulted in 3:1 compounds which crystallise as hydrates.  $TSMnI ((C_3NO_2H_7)_3MnI_2 \cdot 2H_2O)$  and  $TSMgB ((C_3NO_2H_7)_3MgBr_2 \cdot 2H_2O)$  form a second structure type which is a slight variation on the TSCC structure (Figure 7). In both cases, the 3:1 ratio of sarcosine to metal halide is maintained but with the addition of two water molecules per formula unit. The space group and pseudo-hexagonal symmetry of TSCC are both preserved and the unit cell parameters remain similar to the parent compound, but with elongation along the  $b$  axis to accommodate the additional water molecules (Table 1). Interestingly, the M-O polyhedra are linked in a slightly different way from the original compound (Figure 10). In TSCC, each of the metal centres is linked to the next *via* three sarcosine molecules, which act as bridging ligands. In both of these new derivatives, each of the metal centres is only linked to its neighbour by one sarcosine molecule. Each  $M^{2+}$  has six-fold coordination but is coordinated to only four sarcosine molecules and two additional water molecules. Despite the substantial change in connectivity, the three dimensional structure remains interconnected by hydrogen bonding through the N-H...I/Br bonds, with each halide ion forming three hydrogen bonds to sarcosine molecules.

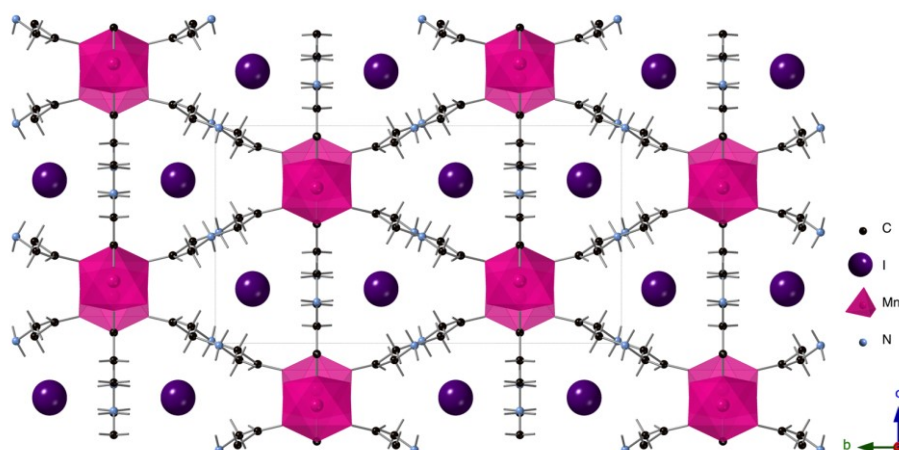


**Figure 7** Structure of TSMnI  $((C_3NO_2H_7)_3MnI_2 \cdot 2H_2O)$  viewed along the  $a$  axis

### 3. Hydrated 2:1 compositions

The incorporation of  $MnCl_2$ ,  $MgCl_2$  and  $CaI_2$  resulted in a third structure type with a different stoichiometry. The structures adopt a 2:1 ratio of sarcosine to metal halide with the incorporation of two water molecules. The structure of BSMnC  $((C_3NO_2H_7)_2MnCl_2 \cdot 2H_2O)$  has been previously reported by Rzaczyńska et al<sup>16</sup> but two new isostructural compounds BSMgC  $((C_3NO_2H_7)_2MgCl_2 \cdot 2H_2O)$  and BSCI  $((C_3NO_2H_7)_2CaI_2 \cdot 2H_2O)$  have been synthesised here (Figure 8). These compositions crystallise in the triclinic system and the pseudo-hexagonal symmetry has been lost. Each of the metal centres has six fold coordination. The sarcosine molecules act as bridging ligands, with two sarcosines connecting each metal centre to the next to form infinite chains along the  $a$  axis and each of the  $Ca^{2+}$  atoms coordinated to two water molecules. DSC data for each of the three compositions did not reveal evidence of any additional phase transitions down to 103 K.

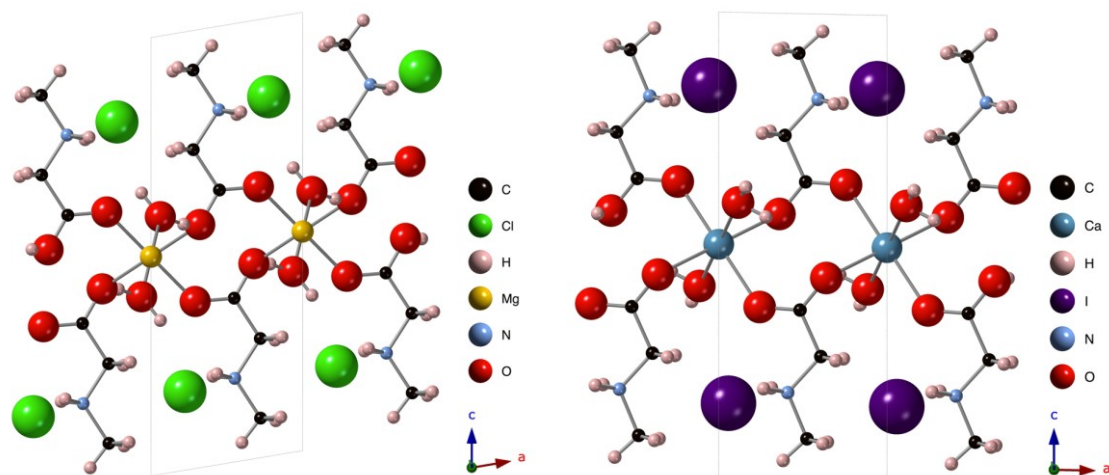


**Figure 8** Structures of BSMgC  $((C_3NO_2H_7)_2MgCl_2 \cdot 2H_2O)$  and BSCI  $((C_3NO_2H_7)_2CaI_2 \cdot 2H_2O)$  viewed along the  $b$  axis

### 4. Hydrated 4:1 Compositions

A second structure type also incorporating  $CaI_2$  was synthesised, TSCI  $((C_3NO_2H_7)_4CaI_2 \cdot 2H_2O)$ . The compound crystallises in the monoclinic crystal system and the original pseudohexagonal symmetry has been lost (Figure 9). The coordination of the  $Ca^{2+}$  remains at six, each is coordinated to two bridging sarcosines, two non-bridging sarcosines and two water molecules. The bridging sarcosines form an infinite chain along the  $b$  axis, again the structure is held together through N—H—X hydrogen bonding

with iodide forming two weak hydrogen bonds to the neighbouring nitrogen atoms of the sarcosines. The only other reported sarcosine metal halide with a 4:1 ratio is diaquaiddodotetrasarcosinepotassium ( $[\text{K}(\text{C}_3\text{H}_7\text{NO}_2)_4]\cdot 2\text{H}_2\text{O}$ ) but its structure differs significantly from that of TSCI.<sup>17</sup> Whilst both 2:1 and 4:1 compositions have been synthesised, so far it has not been possible to synthesise either the hydrated or anhydrous 3:1 complexes incorporating  $\text{CaI}_2$ .

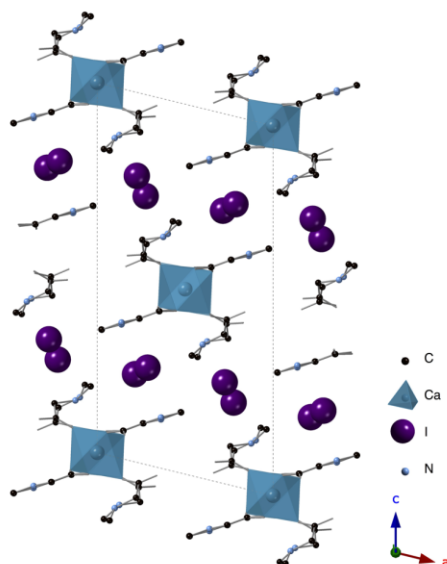


**Figure 9** Structure of TSCI ( $(\text{C}_3\text{NO}_2\text{H}_7)_4\text{CaI}_2\cdot 2\text{H}_2\text{O}$ ) viewed along the *b* axis

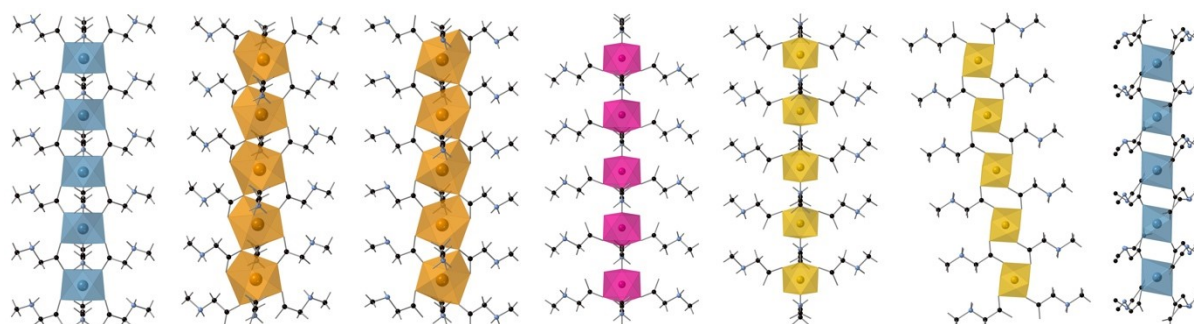


**Figure 10** The chains in sarcosine metal halides a) TSCB ( $(\text{C}_3\text{NO}_2\text{H}_7)_3\text{CaBr}_2$ ) b) TSSC ( $(\text{C}_3\text{NO}_2\text{H}_7)_3\text{SrCl}_2$ ) c) TSSB ( $(\text{C}_3\text{NO}_2\text{H}_7)_3\text{SrBr}_2$ ) d) TSMnI ( $(\text{C}_3\text{NO}_2\text{H}_7)_3\text{MnI}_2\cdot 2\text{H}_2\text{O}$ ) e) TSMgB ( $(\text{C}_3\text{NO}_2\text{H}_7)_3\text{MgBrI}_2\cdot 2\text{H}_2\text{O}$ ) f) BSMgC ( $(\text{C}_3\text{NO}_2\text{H}_7)_2\text{MgCl}_2\cdot 2\text{H}_2\text{O}$ ) g)  $(\text{C}_3\text{NO}_2\text{H}_7)_4\text{CaI}_2\cdot 2\text{H}_2\text{O}$

Figure 10 summarises the arrangements of metal-sarcosine chain units characteristic of each structure type. Our eight newly synthesised sarcosine metal halides are summarised in Table 3 combined with the three previously known structures. New sarcosine metal halide complexes have been synthesised for all of the attempted combinations. For each metal halide combination, a range of reaction conditions and reactant ratios were attempted, however, for certain combinations only 2:1 or 4:1 complexes could be synthesised. Syntheses incorporating  $\text{MnBr}_2$ ,  $\text{MgI}_2$ ,  $\text{SrI}_2$ ,  $\text{BaCl}_2$  and  $\text{BaI}_2$  are yet to be attempted.

**Table 3** Summary of previously known and newly synthesised sarcosine metal halides

Halide	Divalent Metal				
	Mn	Mg	Ca	Sr	Ba
Cl	$(\text{C}_3\text{NO}_2\text{H}_7)_2\text{MnCl}_2\cdot 2\text{H}_2\text{O}^{16}$	$(\text{C}_3\text{NO}_2\text{H}_7)_2\text{MgCl}_2\cdot 2\text{H}_2\text{O}$	$(\text{C}_3\text{NO}_2\text{H}_7)_3\text{CaCl}_2^8$	$(\text{C}_3\text{NO}_2\text{H}_7)_3\text{SrCl}_2$	
Br		$(\text{C}_3\text{NO}_2\text{H}_7)_3\text{MgBr}_2\cdot 2\text{H}_2\text{O}$	$(\text{C}_3\text{NO}_2\text{H}_7)_3\text{CaBr}_2$	$(\text{C}_3\text{NO}_2\text{H}_7)_3\text{SrBr}_2$	$(\text{C}_3\text{NO}_2\text{H}_7)_3\text{BaBr}_2^{18}$
I	$(\text{C}_3\text{NO}_2\text{H}_7)_3\text{MnI}_2\cdot 2\text{H}_2\text{O}$		$(\text{C}_3\text{NO}_2\text{H}_7)_2\text{CaI}_2\cdot 2\text{H}_2\text{O}$		

## Conclusions

We have attempted the synthesis of a wide range of sarcosine metal halide complexes by slow evaporation from aqueous solution, with the aim of preparing new ferroelectrics related to the archetype TSCC. Several new compounds have been prepared in the form of high quality crystals. However, even small changes to the composition and crystal structure result in a loss of the ferroelectric properties seen in the parent compound TSCC. It should be noted that our measurements were limited to a lowest temperature of 90 K and there could be additional phase transitions below this temperature. The thermal decomposition of several of the sarcosine metal halide complexes was monitored using thermal gravimetric analysis revealing a multi-step decomposition with the initial degradation step corresponding to water loss in the hydrated complexes. The formation of different structure types arises from the variations in the sizes of the metal cation and halide. The inclusion of larger cations tends to lead to an increase in the coordination of the metal centres, as seen in both strontium-containing derivatives and the known compound  $(C_3NO_2H_7)_3BaBr_2$ , which have seven and nine-fold coordination, respectively. Hydrated compounds with a 2:1 rather than 3:1 sarcosine:metal-halide ratio are favoured by the inclusion of smaller metal cations. The apparently subtle compositional or crystal-chemical reasons for the occurrence of the unusual ferroelectric behaviour seen in TSCC itself remain to be further explored.

## Acknowledgements

We would like to thank Mrs Sylvia Williamson and Dr Gavin Peters for their help in collecting thermal analysis data and the EPSRC for provision of a doctoral studentship to RC (DTG012 EP/K503162-1).

Supporting information: crystallographic details of the low temperature single crystal refinements, TGA data and further DSC data.

Single crystal X-ray diffraction data for all refinements have been deposited: CDS deposition numbers 1841201-1841219.

The research data pertaining to this paper are available at [xxxxxx](#)

## References

- 1 W. Zhang and R. Xiong, *Chem. Rev.*, 2012, **112**, 1163–1195.
- 2 M. E. Lines and A. M. Glass, in *Principles and Applications of Ferroelectrics and Related Materials*, Oxford Scholarship Online, Oxford, 2001, pp. 1–43.
- 3 T. Hang, W. Zhang, H.-Y. Ye and R.-G. Xiong, *Chem. Soc. Rev.*, 2011, **40**, 3577.
- 4 J. Valasek, *Phys. Rev.*, 1921, **17**, 475–481.
- 5 P.-P. Shi, Y.-Y. Tang, P.-F. Li, W.-Q. Liao, Z.-X. Wang, Q. Ye and R.-G. Xiong, *Chem. Soc. Rev.*, 2016, **45**, 3811–3827.
- 6 M. Fleck and A. M. Petrosyan, in *Salts of Amino Acids: Crystallization, Structure and Properties*, 2014, pp. 139–206.
- 7 Y. Makita, *J. Phys. Soc. Japan*, 1965, **20**, 2074–2080.
- 8 T. Ashida, S. Bando and M. Kakudo, *Acta Crystallogr. Sect. B Struct. Crystallogr. Cryst. Chem.*, 1972, **28**, 1560–1565.
- 9 N. Mishima, K. Itoh and E. Nakamura, *Acta Crystallogr. Sect. B Struct. Crystallogr. Cryst. Chem.*, 1984, **C40**, 1824–1827.
- 10 S. P. P. Jones, D. M. Evans, M. a. Carpenter, S. a. T. Redfern, J. F. Scott, U. Straube and V. H. Schmidt, *Phys. Rev. B*, 2011, **83**, 094102.

- 11 M. Fujimoto, S. Jerzak and W. Windsch, *Phys. Rev. B*, 1986, **34**, 1668–1676.
- 12 J. F. Scott, F. D. Morrison, A. M. Z. Slawin, P. Lightfoot, R. Clulow, A. S. A. Gherson, A. M. Bumstead, J. Gardner, S. C. Capelli, M. R. Probert, S. Sahoo, J. S. Young, R. S. Katiyar and E. K. H. Salje, *Phys. Rev. B*, 2017, **95**, 094119.
- 13 S. Fujimoto, N. Yasuda and H. Kashiki, *J. Phys. D. Appl. Phys.*, 1984, **17**, 1019–1028.
- 14 S. Fujimoto, N. Yasuda and H. Kashiki, *J. Phys. D. Appl. Phys.*, 1982, **15**, 487–495.
- 15 T. Hikita and T. Maruyama, *J. Phys. Soc. Japan*, 1992, **61**, 2840–2847.
- 16 Z. Rzaczyńska, R. Mrozek and M. Sikorska-Iwan, *Pol. J. Chem.*, 2002, **76**, 29–35.
- 17 M. Fleck, V. V. Ghazaryan and A. M. Petrosyan, *Acta Crystallogr. Sect. C Cryst. Struct. Commun.*, 2013, **69**, 11–16.
- 18 M. Trzebiatowska-Gusowska, A. Gągor, J. Baran and M. Drozd, *J. Raman Spectrosc.*, 2009, **40**, 315–322.